

New Analytical Approach for Reservoir Stress Approximation Based on Acid Fracturing Data

Haghi A.H.; Dept. of Petroleum Eng., NISOC, Ahwaz

Kharrat R.; Petroleum University of Technology

*Asef M.R.; Faculty of Earth Sciences, Kharazmi University, Tehran, Iran

Received: 3 Sep 2013

Revised: 11 Nov 2014

Abstract

In this research attempts were made to estimate the in-situ stresses acting on a hydrocarbon reservoir based on routine activities of acid injection in oil reservoir. It was found that the relation between the re-opening pressure of fracture and principal in-situ stresses can be estimated using rock mechanics equations for the circular underground cavities. An appropriate relation between the maximum and minimum horizontal principal in-situ stresses and reservoir parameters such as permeability, reservoir pressure, Young's modulus, acid viscosity, injection flow rate and etc., was developed by using the well-known Darcy equations for fluid flow in porous media. Accordingly, knowing the flow rate of acid injection during well operations and some other reservoir parameters, in-situ stresses may be estimated. The method was then successfully applied to a large carbonate reservoir as a case study in south-west of Iran. Maximum and minimum effective horizontal stresses were calculated by employing the presented method.

Keywords: Rock mechanic; Acid fracturing; Re-opening pressure; In-situ stresses.

*Corresponding author

asef@khu.ac.ir

1. Introduction

In-situ stresses acting on a hydrocarbon reservoir are essential characteristics to be known before any geomechanical evaluation is completed. Knowledge of stress at smaller basin and field scales has critical importance for petroleum applications such as wellbore stability, and reservoir compaction [1-3]. Although some methods have been introduced for direct measurement of these stresses, practical limitations such as finance, time, and accessibility at the time data is required, encourage industry to seek for alternative options. In general, two different approaches may be followed for this purpose. First, laboratory experiments on core specimens such as differential strain core analysis DSCA [4], differential wave velocity analysis, DWVA [5], and an elastic strain recovery (ASR). These methods can be used if the direction core specimens are known [6, 7]. Second, field approaches based on down hole measurement as follows seem to be more reliable, but also more expensive:

- Hydraulic fracturing [8],
- Study borehole break-outs and subsequent elongation plus the natural fracture pattern around the borehole by well logs like caliper log [9,10],
- Study drilling induced tensile fractures by formation micro imager, FMI, and/or borehole tele-viewer logging, BHTV [11-13],
- Over coring and focal mechanism [14-16]

Further information on the subject could be viewed also in the related literature such as Fjaer et al. [17] and Zoback [18].

Furthermore, accumulation of data in oil-rich states encouraged some authors to determine the magnitude of the in situ stresses. Reynolds et al. [19] determined the magnitude of the in situ stresses in the Cooper-Eromanga Basins using an extensive petroleum exploration database from over 40 years of drilling. They calculated the vertical stress based on density and velocity check-shot data and used leak-off test data for estimation of the lower bound of minimum horizontal stress magnitude, and closure pressures from a large number of minifrac tests for estimation of the minimum horizontal stress. They reported that the magnitude of the maximum horizontal stress was constrained by the frictional limits to stress beyond which faulting occurs and by the presence of drilling-induced tensile fractures in some wells. Raaen et al [20] promoted the current extended LOT for estimation of minimum horizontal stress by adding a monitored flowback phase. With respect to hydraulic fracturing and Hydraulic test on pre-existing fracture a full explanation was presented as ISRM suggestions by Haimson and Cornet [21]. Still fracturing technologies have inefficiency in S_H estimation in oil fields [22].

In this research, acid fracturing method is presented as a stress indicator. An appropriate relation between the maximum and minimum horizontal principal in-situ stresses and reservoir parameters such as permeability, reservoir pressure, Young's modulus, acid viscosity,

injection flow rate and etc, was developed by using the well known Darcy equations for fluid flow in porous media. Through presented method in this research, breakdown pressure is substituted by reopening pressure in order to eliminate inaccuracies in detecting breakdown pressure.

Knowledge of the present-day stress orientation is particularly important in Iran, which has an extensive and mature petroleum exploration and production industry. Yet, the 2008 World Stress Map database contains very little present-day stress information for Iran and no stress data from petroleum wells [23]. Yaghoubi and Zeinali [24] investigated a detailed profile of the stress orientation in two wells in the Cheshmeh Khush oilfield in SW of Iran. Later, Rajabi et al. [25] examined resistivity image logs and determined the present-day stress orientation of the Abadan Plain in SW Iran. Recently, Haghi et al. [26] conducted an analysis of the present day stress of the central Persian Gulf using full-bore FMI log, leak of test and density logs. By creating the first full stress tensor, they concluded a strike-slip stress regime in the studied area in the South of Iran. These researches indicated that the stresses in South and South-West of Iran are linked to the resistance forces generated by the Arabia – Eurasia collision at the Zagros orogeny.

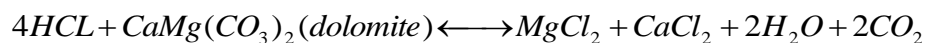
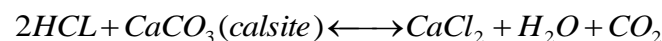
In this paper, present day insitu stress is investigated based on acid fracturing data for a carbonate reservoir in SW of Iran. Using this method, maximum and minimum effective horizontal stresses are

calculated. The calculated minimum horizontal stress is compared with leak-off pressure, and this comparison validates the accuracy of the introduced method.

2. Acidizing Process and Insitu Stress

Acids are used as fracture fluids, for scale removal as well as matrix treatments. Acids are also used to clean up gravel packs once they are positioned, or as cleansing agents to preflush the formation prior to administering a near-wellbore chemical treatment. Acid systems in current use can be classified as mineral acids, dilute organic acids, powdered organic acids, hybrid (or mixed) acids and retarded acids. All acids with the exception of hydrochloric-hydrofluoric and formic-hydrofluoric acid mixtures are used to treat carbonate formations. It is, with few exceptions, generally necessary to include hydrofluoric acid (HF) in treatment of sandstones [27].

In addition to HCL there are other organic acids used to treat carbonate formation, HCL is one of the most ordinary in acidizing. As a result, in this paper only the typical reactions of HCL are mentioned as follows:



Acidizing treatments in sandstone formations normally employ a mixture of HCL and HF. This acid mixture is used because HF is

reactive with clay minerals and feldspars that may be restricting the permeability near the wellbore.

2.1. Acid Fracturing:

In oil industry acidizing is a well-known method for well stimulation. Accordingly, creating a fracture by an acid fluid in an area around the well will effectively remove the skin effect. As a result, hydrocarbon will bypass the damages zone through fractures rather than crossing through porous media. Therefore, the permeability of the area around the well will increase, pressure drop related to skin effect turns to negative value and consequently the productivity index of reservoir will increase. The following equation is typically used for analysis of the this process[28]:

$$PI = \frac{(k_s/k) \ln(r_e/r_w)}{\ln(r_s/r_w) + (k_s/k) \ln(r_e/r_s)} \quad (1)$$

As a result of well stimulation, PI becomes greater than one, which implies better operation of reservoir (eq.1).

2.2 Relation between in-situ stresses and re-opening pressure

In order to create a fracture, RTTS packers are used to isolate a limited length of the borehole from the rest of the well. Then the fluid is injected into the section between the packers. Due to increasing of pressure, the rock will eventually break. The orientation of minimum principal stress is perpendicular to fracture plane as illustrated in Figure1. In order to recognize this orientation, certain inflatable packers which can record this orientation may be employed. In case,

inflatable packers are not available, the orientation can be determined after fracturing by using Image logs like FMI, UBI etc.

The objective of this research is to determine the stress magnitude using re-opening pressure. The fracturing process follows the steps presented in Figure2. First of all, the pressure is increased until it exceeds the breakdown pressure and at this moment a fracture initiates at the borehole (first pick, P_b). Accordingly, the pressure sharply decreases due to fluid loss through the opened fracture. Shutting down the fluid pumping into the well, the pressure curve reclines but not very sharp due to existence of insitu stresses. This will continue until insitu stresses close the created fracture. The pressurizing process is repeated, but at the lower value than the first stage. Therefore, the second pick is obtained at a lower pressure. This pressure is termed as the re-opening pressure (P_{ro}).

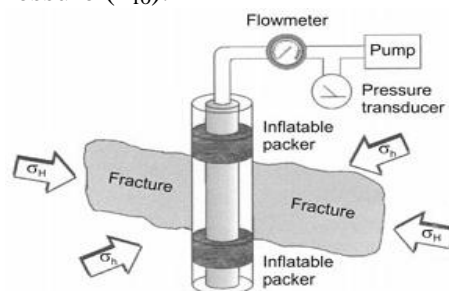


Figure1. Stages of starting hydraulic fracture test and the position of principle stresses to fracture plane [29]

It should be noted that in the first opening, part of the fluid pressure will be used to overcome the tensile strength (σ_t) of rock and this tensile strength depends on the rock type (eq.2).

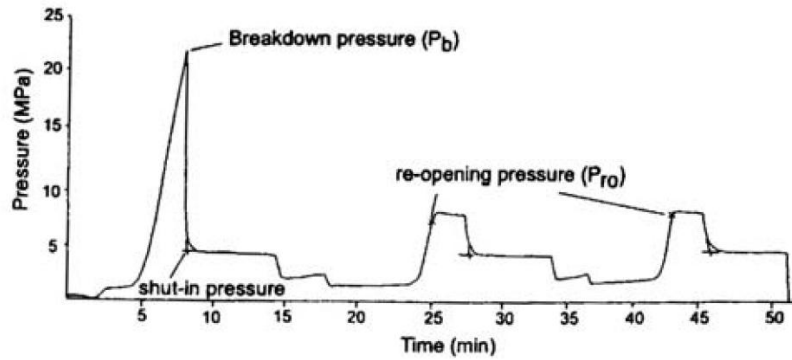


Figure 2. Stages of creating a hydraulic fracture [12]

$$P_b - \sigma_t = P_{ro} \quad (2)$$

However, re-opening pressure will be used to overcome in-situ stresses of rock, only. Of course, if the formation is naturally fractured, then the difference between the first opening pressure and the re-opening pressure may reduce substantially. Otherwise, re-opening could be accurately used as an approximation of the first opening pressure.

As it is known, to keep the fracture open during the fracture propagation, the pressure inside the fracture must overcome the minimum insitu stress. Accordingly, the pressure inside the fracture must be approximated accurately. Daneshi [12] found that in order to determine the real minimum stress, the average of pressure along the fracture must be obtained where the average pressure starts from the existing pressure in wellbore to the existing pressure at the tips of the fracture. As it is illustrated in Figure 3 [30], the pressure curve along the fracture is indicated by a line with high tangent. However, since the pressure was relatively constant during the entire injection period,

the data for 108 seconds of injection time was used to compare the average pressure inside the fracture with its value at the wellbore. In this case the amount of pressure inside the fracture along a certain length of fracture (2.2-3 ft) remains stable and curve tangent reaches almost zero. The pressure in this area can be considered as the average pressure.

As it is illustrated in Figure3 (fracture in a rectangular shape fracture,) the magnitude of the average fracture pressure for the graph of 108 second estimates 304 psi ($P/P_{ro} = 0.76$). This indicates that the average pressure inside the fracture (whose amount is almost equal to the minimum stress) is 24% less than the re-opening pressure (400 psi), i.e. the magnitude of minimum stress is about 24% less than the re-opening pressure. Therefore, in this special case this amount is the real upper limit for the minimum in-situ stress.

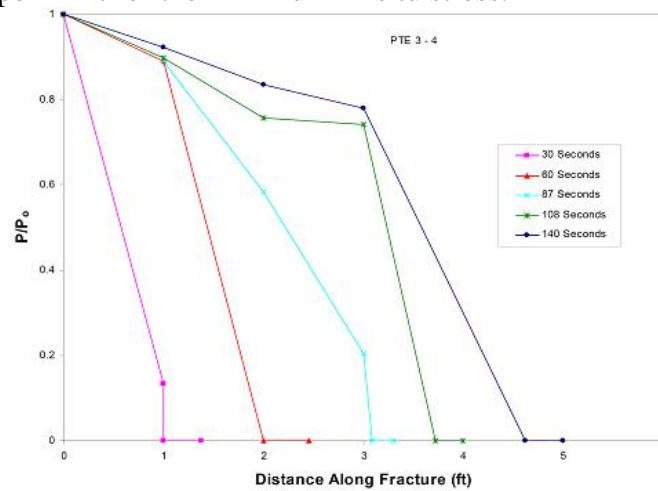


Figure3. Fluid pressure variations inside the fracture (P_0 is the pressure inside the well, P is pressure inside the fracture) [30]

Using rock mechanics equations, minimum and maximum effective stresses are extrapolated based on the re-opening pressure. For this purpose, the solution proposed by Kirsch [31] regarding stress distribution for circular drillings in polar coordinate is applied (Figure 4). Further equations (eq's 3, 4 and 5) could be seen in the related literature such as Fjaer et al [32], Fjaer et al [17] and also [33].

$$\sigma_r = \frac{P}{2} \left\{ (1+k) \left(1 - \frac{a^2}{r^2} \right) - (1-k) \left(1 - \frac{4a^2}{r^2} + \frac{3a^4}{r^4} \right) \cos 2\theta \right\} \quad (3)$$

$$\sigma_\theta = \frac{P}{2} \left\{ (1+k) \left(1 + \frac{a^2}{r^2} \right) - (1-k) \left(1 + \frac{3a^4}{r^4} \right) \cos 2\theta \right\} \quad (4)$$

$$\tau_{r\theta} = \frac{P}{2} \left\{ (1-k) \left(1 + \frac{2a^2}{r^2} - \frac{3a^4}{r^4} \right) \sin 2\theta \right\} \quad (5)$$

Where θ is measured from the azimuth of minimum horizontal stress (Figure 4). In these equations, replacing "r" with well radius "a" the effective stresses on the borehole will be obtained as presented in eq's 6, 7 and 8:

$$\sigma_r = 0 \quad (6)$$

$$\sigma_\theta = P \{ (1+k) + 2(1-k) \cos 2\theta \} \quad (7)$$

$$\tau_{r\theta} = 0 \quad (8)$$

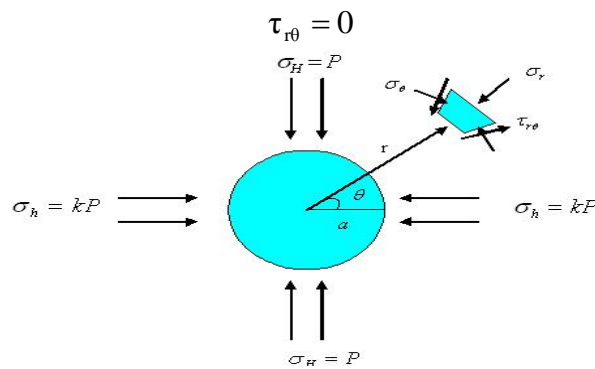


Figure 4. Stress distribution around a circle drilling

Through fracturing at the borehole wall ($r = a$), acid injection pressure should overcome to the tangential stress in the direction of maximum horizontal stress which has least stress concentration ($\theta = 0$ and 180). Accordingly, the minimum horizontal stress oriented perpendicularly on $\theta = 90$ and 270 (eq.'s 9 and 10). Therefore the magnitude of the tangential stresses in wellbore in the direction of maximum and minimum stresses is measured as follow,

$$\theta = 0 \rightarrow \sigma_{\theta} = P(3 - k) \quad (9)$$

$$\theta = 90 \rightarrow \sigma_{\theta} = P(3k - 1) \quad (10)$$

For a vertical well drilled parallel to the vertical stress, P could be substituted by σ_H in eq. 10. Hence, the eq. 10 changes to eq. 11 as follow:

$$\frac{\sigma_{\theta}}{\sigma_H} = 3k - 1 \quad (11)$$

Sheorey [34] developed an elasto-static thermal stress model of the earth. This model considers curvature of the crust and variation of elastic constants, density and thermal expansion coefficients through the crust and mantle. He did provide a simplified equation which can be used for estimating the ratio of minimum to maximum stress k . This equation is:

$$K = 0.25 + 7E_h \left(0.001 + \frac{1}{z} \right) \quad (12)$$

Where z (m) is the depth below surface and E_h (GPa) is the average deformation (Young's) modulus of the upper part of the

earth's crust measured in a horizontal direction. A plot of this equation is given in Figure 6 for a range of deformation modulus.

Herein, eq. 12 is used as an acceptable approximation for K value into eq. 11 as follow,

$$\sigma_{\theta} = (3(0.25 + 7E_h(0.001 + \frac{1}{Z})) - 1)\sigma_H \quad (13)$$

Eq. 13 is simplified to eq. 14.

$$\sigma_{\theta} = (21E_h(0.001 + \frac{1}{Z}) - 0.25)\sigma_H \quad (14)$$

The tangential stress in eq. 14 must be equal to first opening pressure minus tensile strength of the rock during acid fracturing. Otherwise, it must be replaced by re-opening pressure base on eq. 2. upon Sheorey's equation [34].

$$P_{ro} = (21E_h(0.001 + \frac{1}{Z}) - 0.25)\sigma_H \quad (15)$$

Now by using eq. 15, the relation between maximum in-situ stress and re-opening pressure is defined in eq. 16.

$$\sigma_H = (\frac{1}{21E_h(0.001 + \frac{1}{Z}) - 0.25})P_{ro} \quad (16)$$

Using the definition of K value as presented in eq. 17, the minimum horizontal effective stress specified from eq. 16 as provided in eq. 18.

$$K = \frac{\sigma_h}{\sigma_H} \quad (17)$$

$$\sigma_h = (\frac{0.25 + 7E_h(0.001 + \frac{1}{Z})}{21E_h(0.001 + \frac{1}{Z}) - 0.25})P_{ro} \quad (18)$$

For more clarification, eq. 18 is rearranged to eq. 19.

$$\sigma_h = \left(1 + \frac{1}{21E_h \left(0.001 + \frac{1}{z}\right) - 0.25}\right) \frac{p_{ro}}{3} \quad (19)$$

Therefore, the magnitude of minimum and maximum stresses could be determine simply using the re-opening pressure, deformation modulus (young's module) and depth as summarized in eq.'s 20 and 21.

$$\sigma_h = B \times p_{ro} \quad (20)$$

$$\sigma_H = A \times p_{ro} \quad (21)$$

While $A = \frac{1}{21E_h \left(0.001 + \frac{1}{z}\right) - 0.25}$ and $B = (1 + A)/3$.

Figure5 displays the variations of A and B (re-opening pressure coefficient for maximum and minimum in-situ stresses, respectively) parameters with young's modulus.

Now, Daneshi's lab results on the relation between minimum horizontal stress and re-opening pressure is converted to specify the relation between maximum horizontal stress and re-opening pressure as presented in eq.'s 22 to 25. :

$$p_{ro} = 3\sigma_h - \sigma_H \quad (22)$$

$$p_{ro} = 3(0.76p_{ro}) - \sigma_H \quad (23)$$

$$\sigma_h = 0.76p_{ro} \quad (24)$$

$$\sigma_H = 1.28p_{ro} \quad (25)$$

Now comparing eq.'s 24 and 25 with eq.'s 20 and 21 for a vertical well, the value of Young's modulus for the Daneshi's test at a certain depth of 2000 m becomes 33 GPa.

It is known that 90% of host rocks for oil reservoirs around the world are limestone, dolomite and sandstone. Correspondingly there are some typical amounts of young's modulus as shown in Table 1.

Table 1. Typical values for Young's modulus [35]

Material	Sandstone	Limestone	Dolomite	Shale	Granite
Young's Modulus (GPa)	0-55	30-80	40-70	0-80	50-90

2.3 Integrating reservoir parameters

The value of re-opening pressure in Figure 2 can be directly extracted from the vertical axis. However, the following equation [28] can be used in this regard, as well [36].

$$P_{wf} - P_R = \frac{j\mu}{7.08kh} \left[\ln\left(\frac{r_c}{r_w}\right) - \frac{3}{4} \right] \quad (26)$$

Eq. 26 specifies the relation between the pressure at the bottomhole and flow rate of acid injection in form of matrix acid treatment based on Darcy fluid flow definitions. In this equation, bottomhole pressure,

P , and the flow rate of acid injection, j , are directly related to each other. It should be noted that these values are obtained during the preliminary studies of the reservoir.

In fact, acidizing in oil wells is performed in two ways: the first, is matrix acid treatment in which the purpose is not breaking the formation. Rather, the objective is damage removal by resolving them of the way of hydrocarbon flow. The second method is acid fracturing

in the wellbore in order to bypass the damage zone around the well. Therefore, eq. 26 specifies the relation between bottomhole pressure and the injection flow rate before fracture initiation. Above such pressure (in acid fracturing), there is no direct relation between these two parameters. Accordingly before critical flow rate ($j_{critical}$) the relation between j and P_{wf} is linear with a positive gradient (that obeys equation 26). Then, as a result of fracturing, the pressure decreases. Therefore, eq. 26 is no longer applicable. In fact, $j_{critical}$ for matrix acidizing operation is j_{max} , while the same value for acid fracturing operation is j_{min} . Therefore, $j_{critical}$ is the critical parameter. At this point, fracturing in wellbore initiates and the pressure inside wellbore becomes equal to the re-opening pressure. If the pressure on the bottomhole is equalized to the re-opening pressure ($P_{wf} = P_{ro}$), eq. 26

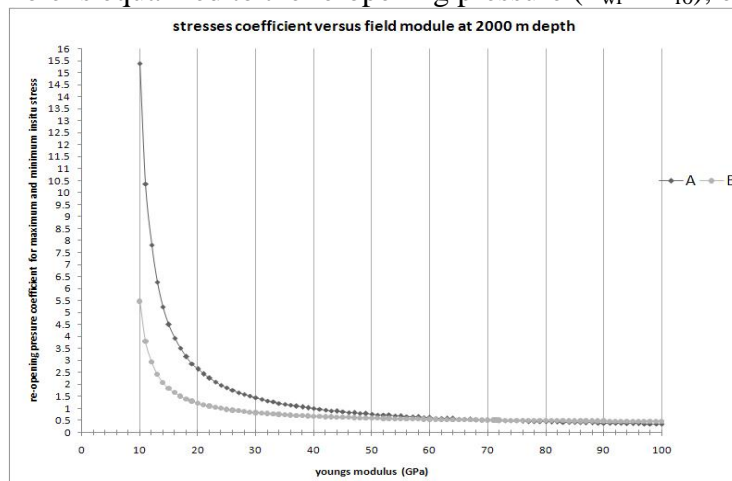


Figure 5. Stress coefficient versus Horizontal young's modulus at 2000 m depth oil reservoir

turns to eq. 278.

$$P_{ro} - P_R = \frac{j_{critical}\mu}{7.08kh} \left[\ln\left(\frac{r_e}{r_w}\right) - \frac{3}{4} \right] \quad (27)$$

By inserting eq.'s 20 and 21 into eq. 27, the magnitude of in-situ stresses could be measured in oil unit system (eq. 29 and 30).

$$\sigma_h = BP_R + \frac{j_{critical}B\mu}{7.08kh} \left[\ln\left(\frac{r_e}{r_w}\right) - \frac{3}{4} \right] \quad (28)$$

$$\sigma_H = AP_R + \frac{j_{critical}A\mu}{7.08kh} \left[\ln\left(\frac{r_e}{r_w}\right) - \frac{3}{4} \right] \quad (29)$$

In these equations, A and B are dimensionless coefficients but the parameters inside these coefficient have SI unite. Accordingly, eq.'s 28 and 29 could be extended in oil unit system as follows:

$$\sigma_h = \frac{1}{3} \left(1 + \frac{1}{E_h \times 10^{-5} (0.01447 + \frac{47.49}{z}) - 0.25} \right) P_R + \frac{j_{critical} (0.75 + E_h \times 10^{-5} (0.01447 + \frac{47.49}{z})) \mu}{21.24 (E_h \times 10^{-5} (0.01447 + \frac{47.49}{z}) - 0.25) kh} \left[\ln\left(\frac{r_e}{r_w}\right) - \frac{3}{4} \right]$$

$$\sigma_H = \left(\frac{1}{E_h \times 10^{-5} (0.01447 + \frac{47.49}{z}) - 0.25} \right) P_R + \frac{j_{critical}\mu}{7.08 (E_h \times 10^{-5} (0.01447 + \frac{47.49}{z}) - 0.25) kh} \left[\ln\left(\frac{r_e}{r_w}\right) - \frac{3}{4} \right]$$

Where young's modulus and depth are represented into psi and ft, respectively.

3. A Case Study in SW of Iran

The Field "A" in SW of Iran has been in production since 1959. This field, one of the largest hydrocarbon-bearing structures in the world, is a large northwest-southeast-trending anticline with a subsurface area of 80 by 10.5 km (Figure6). This field has 14 active reservoir layers, eight sandstone units and six carbonate units. The

main units at the field are high-porosity and high-permeability, siliciclastic-rich units that serve as flow conduits. In contrast, the carbonate-rich units, which exhibit lower average porosities and permeability's, behave as relative baffles to fluid flow. The shale units act as fluid barriers. The lower to upper Cretaceous formation of the Bangestan reservoir in "A" oil field was discovered in 1959 (Figure7). Bangestan reservoir is a carbonate reservoir of 3000 ft thickness. It is entirely composed of limestone.

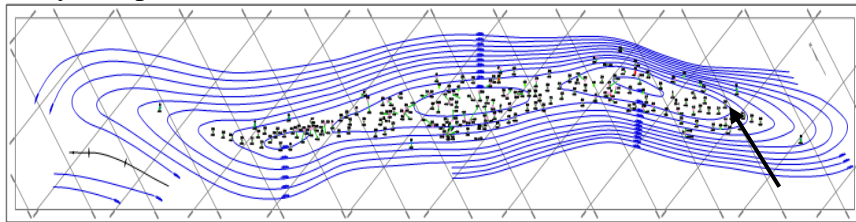


**Figure6. UGC map of Field "A" in SW of Iran
"A"**

A set of well input data as listed in Table 23 is used to demonstrate the validity and sensitivity of the above equation. The objective is to determine the magnitude of in-situ stresses. Well no. 229 is completed into a Ilam reservoir at 3450 m depth from surface level to the top of first perforation depth. The average horizontal Young's modulus for reservoir rock is obtained from acoustic velocity and transition time on core samples equal to 8×10^6 psi.

By using eq.'s 28 and 29, the magnitude of in-situ stresses can be obtained. For this purpose, first the apparent radius of the well (r'_w) needs to be calculated.

Table 2. Real well input data

Parameter	Abbreviation	Value	Dimension
Well radius	R	0.354	ft
Skin factor	S	-5.25	-
permeability	K	0.0062	Darcy
Initial reservoir pressure	P _R	5562	Pisa
Drainage radius	r _e	1100	ft
Acid viscosity	μ	2.5	cp
Thickness	H	207	ft
Critical acid flow rate	j _{critical}	100	bbl/day

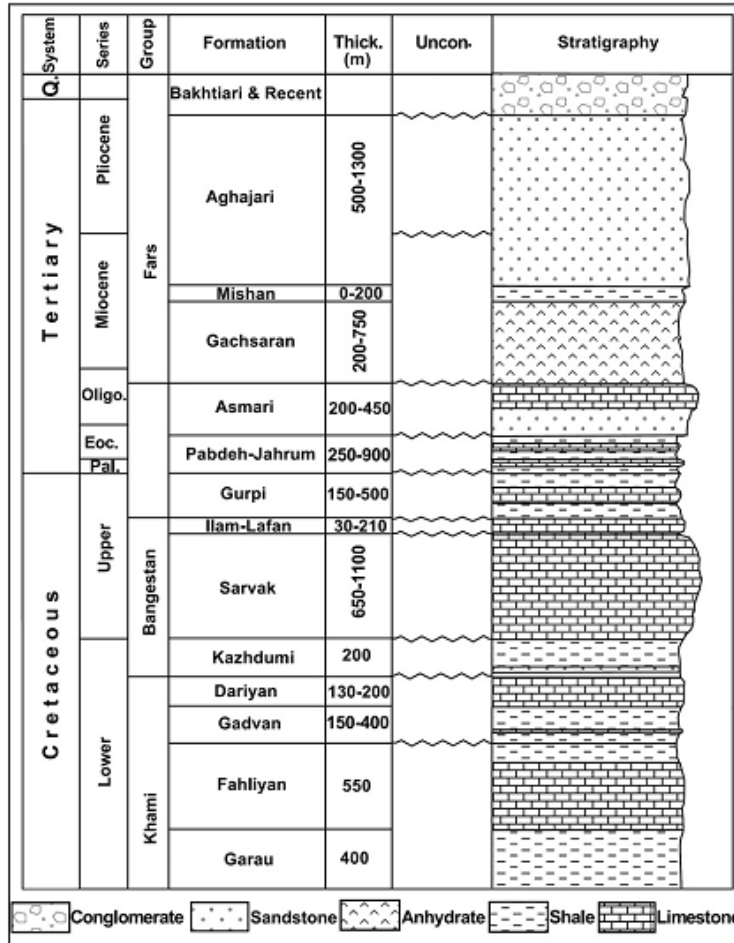


Figure 7. The stratigraphy and thickness of Bangestan reservoir in field

$$r'_w = r_w \exp(-S)$$

$$r'_w = 3.5 \exp(-10) = 52.54 \text{ ft}$$

Now the magnitudes of minimum and maximum effective in-situ stresses are calculated as follows.

$$\sigma_h = BP_R + \frac{j_{\text{critical}} B \mu}{7.08 kh} \left[\ln\left(\frac{r_e}{r'_w}\right) - \frac{3}{4} \right]$$

$$\sigma_h = \frac{1}{3} \left(1 + \frac{1}{80 \times (0.01447 + \frac{47.49}{11318.9}) - 0.25} \right) \times 5562 + \frac{100 \times (0.75 + 80(0.01447 + \frac{47.49}{11318.9})) \times 2.5}{21.24 \times (80 \times (0.01447 + \frac{47.49}{11318.9}) - 0.25) \times 0.0062 \times 207} \left[\ln\left(\frac{1100}{52.53}\right) - \frac{3}{4} \right]$$

And

$$\sigma_H = AP_R + \frac{j_{\text{critical}} A \mu}{7.08 kh} \left[\ln\left(\frac{r_e}{r'_w}\right) - \frac{3}{4} \right]$$

$$\sigma_H = \left(\frac{1}{80 \times (0.01447 + \frac{47.49}{11318.9}) - 0.25} \right) 5562 + \frac{100 \times 2.5}{7.08 \times (80 \times (0.01447 + \frac{47.49}{11318.9}) - 0.25) \times 0.0062 \times 207} \left[\ln\left(\frac{1100}{52.53}\right) - \frac{3}{4} \right]$$

As a result,

$$\sigma_h = 3367 \text{ psi} = 23.21 \text{ MPa}$$

$$\sigma_H = 4478 \text{ psi} = 30.86 \text{ MPa}$$

Calculated effective minimum horizontal stress must be added to reservoir pore pressure to find the insitu principle minimum horizontal stress equal to 8400psi.

To examine the accuracy of the presented method, the calculated values should be compared with some insitu gathered field data. As we know, there is no direct method for determination of maximum horizontal stress on the basis of field data. However, some fracturing

methods are available in oil industries to estimate the minimum horizontal insitu stress directly such as extended leak of test (XLOT). Herein, XLOT data form Field “A” is used to evaluate the accuracy of the presented approach. As it is shown in Figure8, the XLOT graph of wellhead pressure versus time for a well in field “A” represents a value equal to 1754 psi for the fracture shut-in pressure. Converting this value to insitu minimum horizontal stress, it is estimated 8292 psi at 3500 m depth. Fortunately, the difference between the calculated value and field data is negligible.

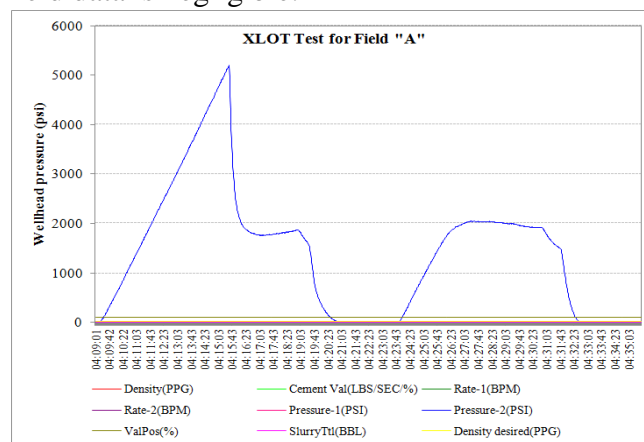


Figure8. XLOT test result for Field "A", SW of Iran. The graph illustrates variation of wellhead pressure versus time at 3500 m depth. Herein, the breakdown and shut-in pressure are resulted equal 11436 and 8292 psi, respectively.

The comparison between the field stresses with calculated values confirms the accuracy of the presented method and all assumed theories including Sheory method for the field “A”.

3.1. Sensitivity Analysis

In eq.'s 28 and 29, the most effective parameter is the reservoir pressure (first parts of right sides of equations (28) and (29)).

$$\sigma_h = 3345 \text{ psi} + 22 \text{ psi} = 3367 \text{ psi}$$

$$\sigma_H = 4474 \text{ psi} + 4 \text{ psi} = 4478 \text{ psi}$$

Other parameters like skin factor, initial permeability, thickness, acid viscosity, well radius and drainage radius are related to the critical flow rate and also to each other. If one of them changes, the other parameters will change consequently. Accordingly, the in-situ stresses are not sensitive by reservoir parameters. This result seems to be reasonable because in fact, in-situ stresses are functions of overburden pressure, tectonic activity pressure and etc., and not of the reservoir parameters.

Nevertheless, two parameter of Young's modulus and depth in eq.'s 28 and 29 affect the magnitude of in-situ stresses.

The relation between in-situ stresses and depth is clear and reasonable. By changing the depth, in-situ stresses should change. For example in the considered reservoir, if depth of reservoir decreases to 2000 m (6561 ft) the magnitude of in-situ stresses becomes:

$$\sigma_h = 3123 \text{ psi} = 21.5 \text{ MPa}$$

$$\sigma_H = 3745 \text{ psi} = 25 \text{ MPa}$$

Furthermore, if the value of the Young's modulus changes to 50×10^5 psi, the magnitudes of in-situ stresses becomes:

$$\sigma_h = 4590 \text{ psi} = 31.64 \text{ MPa}$$

$$\sigma_H = 8147 \text{ psi} = 56.17 \text{ MPa}$$

These values for maximum and minimum horizontal stress demonstrates the sensitivity of stress data with Young's modulus. This result seems logical, because Young's modulus reflects the elastic behavior of rock which transforms overburden stress into horizontal stresses. This is the case especially in stiff carbonates with highly poroelastic behavior.

5. Conclusions

A novel methodology was presented to estimate the magnitude and orientation of maximum and minimum in-situ stresses on the basis of information obtained from preliminary reservoir studies plus well stimulation data. Suggested methodology is helpful in oil industry in case there is no access to the hydraulic fracturing data. While many reservoir parameters such as well radius, skin factor, initial permeability, initial reservoir pressure, drainage radius, acid viscosity, thickness, and critical acid flow rate contribute in the equation, it was demonstrated that only parameters genially related to the matter (namely, reservoir depth and the Young's modulus of rock), affect the in-situ stresses.

For the case of field "A" located in SW of Iran, minimum and maximum horizontal insitu stresses are calculated equal to 3207 and 3997 psi at 3500 m depth. The concluded value for minimum horizontal insitu stress is consistent with XLOT test result. This confirms the accuracy of the presented method and all assumed theories including Sheory method for the field "A", SW of Iran. This

approach can innovatively create significant knowledge regarding the reservoir mechanics, using the routinely available acid fracturing information.

Nomenclatures:

σ_H = maximum horizontal principal in-situ stress (psi)

σ_h = minimum horizontal principal in-situ stress (psi)

P_R = initial pressure of the reservoir (psi)

P_{wf} = pressure of fluid injection (psi)

P_{ro} = re-opening pressure (psi)

P_o = opening pressure (psi)

σ_r = radial stress (psi)

σ_θ = tangential stress (psi)

P = perpendicular stress (psi)

$\tau_{r\theta}$ = shearing stress (psi)

$\dot{J}_{critical}$ = Critical flow rate (bbl/day)

j = Injection flow rate (bbl/day)

μ = fluid viscosity injected into the reservoir (acid viscosity) (cp)

k_s = permeability around the well (which has increased due to fracture) (Darcy)

k = main permeability of the reservoir (Darcy)

r_e = radius of the reservoir drainage (ft)

r_s = radius of stimulation area (ft)

r_w = radius of the well (ft)

r'_w = apparent radius of the well ($r'_w = r_w \exp(-S)$) (ft)

a = well radius (ft)

r = distance between the element under study and the well axis (Figure 5)

(ft)

h = thickness of the reservoir (ft)

S = skin factor

θ = angle of orientation of minimum stress

K = the ratio of minimum and maximum in-situ stress

PI = productivity improvement due to well stimulation

References

1. Tingay M., Muller B., Reinecker J., Heidbach O., Wenzel F., Fleckstein P., "Understanding tectonic stress in the oil patch: the World Stress Map Project", *Lead. Edge* 24 (12) (2005) 1276-1282.
2. Tingay M.R.P., Hillis R.R., Morley C.K., King R.C., Swarbrick E., Damit A.R., "Present-day stress and neotectonics of Brunei: implications for petroleum exploration and production", *AAPG Bull.* 93 (1) (2009) 75-100.
3. Haghi A.H., Kharrat R., Asef M.R., "Simulation and analysis of production induced compaction using Geomechanical formulation of fracturing technology for stress prediction", *Proc. SPE/IPTC*, 14832-pp, Bangkok, Thailand (2011).
4. Ren N.K., Roegiers J.-C. "Differential strain curve analysis-a new method for determining the pre-existing in situ stress state of rock core measurements", *Proc. 5th Int. Conf. of the Int. Soc. of Rock Mechanics*, Melbourne, Australia: (1983) F117-F127.

5. Engelder T., Plumb R., "Changes in In-situ Ultrasonic properties of Rock on strain relaxation", *Int. J. RockMech. Min. Sci. & Geomech.abstr.*21 (1984) 75-82.
6. Blanton T.L., "The relation between recovery deformation and in situ stress magnitudes from anelastic strain recovery of core. SPE/DOE 11624., SPE/DOE Symp. On low permeability, Denver, March (1983) 14-16.
7. Warpinski N.R., Teufel L.W., "A viscoelastic Constitutive Model for determining in situ stress magnitude from Anelastic strain recovery of core", SPE15368, 61st Annual Technical Conference and Exhibition, New Orleans, October (1986) 5-8.
8. Haimson B.C., "Status of in situ stress determination methods", *Proc. 29th U.S. Symp. Rock Mech.* (1988) 75-84.
9. Plump R.A., Hickman S.H., "Stress-induced borehole enlargement: a comparison between the four-arm dipmeter and the borehole televiewer in the Auburn geothermal well", *J. geophys. Res.* 90 (1985) 5513-5521.
10. Zoback M.D., Barton C.A., Brudy M., Castillo D.A., Finkbeiner T., Grollmund B.R., Moos D.B., Peska P., Ward C.D., Wiprut D.J., "Determination of stress orientation and magnitude in deep wells", *Int. J. Rock Mech. & Min. Sci.* 40 (2003)1049-1076.
11. Hayashi K., Shoji T., Niitsuma H., Ito T., Abé H., "A new in situ tectonic stress measurement and its application to a geothermal model field", *Trans. Geother. Resour. Counc.*, Vol.9 (1985) 99-104.

12. Daneshy A.A., "A Study of Inclined Hydraulic Fractures", SPEJ, (1973) 61- 68.
13. Yew C.H., Li Y., "Fracturing of a deviated well", SPE Prod. Engineering (1988) 429-437.
14. Sipkin S.A., "Estimation of earthquake source parameters by the inversion of waveform data", Synthetic waveforms, Physics of Earth and Planetary Interiors. v. 30 (1982) 242-259.
15. Sipkin S.A., "Interpretation of non-double-couple earthquake mechanisms derived from moment tensor inversion", Journal of Geophysical Research, v. 91 (1986) 531-547.
16. Sipkin S.A., "Rapid determination of global moment-tensor solutions", Geophysical Research Letters, v. 21 (1994) 1667-1670.
17. Fjaer E., Holt R.M., Horsrud P., Raaen A.M., Risner R., "Petroleum Related Rock Mechanics 2nd Edition", Elsevier science publishers B.V. ISBN 978-0-444-50260-5 (2008).
18. Zoback M.D., "Reservoir Geomechanics", Cambridge University Press, Cambridge, ISBN-978-0-521-77069-9 (2007).
19. Reynolds S.D., Mildren S.D., Hillis R.R., Meyer J.J., "Constraining stress magnitudes using petroleum exploration data in the Cooper-Eromanga Basins, Australia. Tectonophysics, 415 (1) (2006) 123-140.
20. Raaen A.M., Horsrud P., Kjørholt H., Økland D., "Improved routine estimation of the minimum horizontal stress component from extended leak-off tests". Int. J. Rock Mech. & Min. Sci. 43 (2006) 37-48.

21. Haimson B.C., Cornet F.H., "ISRM Suggested Methods for rock stress estimation-Part3: hydraulic fracturing (HF) and/or hydraulic testing of pre-existing fractures (HTPF)", *Int. J. Rock Mech. & Min. Sci.* 40 (2003)1011-1020.
22. Zoback M.D., "Reservoir geomechanics", Cambridge Press, Cambridge Press (2007).
23. Heidbach O., Tingay M., Barth A., Reinecker J., Kurfeß D., Müller B., "The World Stress Map database release 2008", doi:10.1594/GFZ.WSM.Rel2008 (2008).
24. Yaghoubi A.A., Zeinali M., "Determination of magnitude and orientation of the in-situ stress from borehole breakout and effect of pore pressure on borehole stability-case study in Cheshmeh Kush oilfield of Iran", *J. of Petroleum Science and Engineering* 67 (2009) 116-126.
25. Rajabi M., Sherkati S., Bohloli B., Tingay M., "Subsurface fracture analysis and determination of in-situ stress direction using FMI logs, An example from the Santonian carbonates (Ilam formation) in Abadan Plain, Iran", *J. Tectonophysics*, 492 (2010) 192-200.
26. Hagi A.H., Kharrat R., Asef M.R., "Rezazadegan H., "Present-day stress of central Persian Gulf; Implications for drilling and well performance", *J. Tectonophysics*, doi:10.1016/j.tecto.2013.06.001
Heidbach, O., Tingay, M., Barth, A., Reinecker, J., Kurfeß, D., Müller, B., 2008. The World Stress Map database release 2008. doi:10.1594/GFZ.WSM.Rel2008 (2013).

27. Newell T.P., "In Cellulose Chemistry and Its Applications", Chichester, England: Ellis Harwood Ltd (1985).
28. Dake L.P., "Fundamentals of Reservoir Engineering", Elsevier Ltd London WCIX 8RR (1978).
29. Heidbach O., Tingay M., Barth A., Reinecker J., Kurfec D., Müller B., "Global crustal stress pattern based on the World Stress Map database release 2008 Tectonophysics", 482 (2010) 1-4, 3-15.
30. Warpinski N., "In Situ Measurements of Hydraulic Fracture Behavior- PTE-3 Final Report", Sandia Report SAND83-1826 printed July (1985).
31. Kirsch G., "Die theorie der elastizitat und die bedurfnisse der festigkeitslehre", Veit. Deit. Ing. 42 (28) (1898) 797-807.
32. Fjaer E., Holt R.M., Horsrud P., Raaen A.M., Risner R., "Petroleum Related Rock Mechanics", Elsevier science publishers B.V. (1992).
33. Hadson J.A., Harrison J.P., "Engineer Rock Mechanics: an introduction to principles", Elsevier Science Ltd (1997).
34. Sheory P.R., "A theory for in situ stresses in isotropic and transversely isotropic rock. Int. J. Rock Mech. Min. Sci. & Geomech. Abstr. 31(1) (1994) 23-34.
35. Amadei B., Stephansson O., "Rock Stress and Its Measurement. Published by Chapman & Hall", 2-6 Boundary Row, London SE18HN (1997).
36. McLeod H.O., Ledlow, L.B., Till M.V., "The Planning, Execution and Evaluation of Acid Treatments in Sandstone Formations", SPE 11931, presented at the 58th Fall Technical Conference and Exhibition of the Society of Petroleum Engineers, San Francisco, October (1983).